Research Article

A new extractant impregnated resin for separation of traces of uranium and thorium followed by their spectrophotometric determination in some geological samples

Hisham Fouad[1] · Saeyda Abu Elenein[2] · Ahmed Orabi[1] · Shaimaa Abdulmoteleb[1]

Abstract

A new extractant-impregnated resin, alizarin red S -impregnated XAD-2010, is used as an adsorbent to separate and preconcentrate U(VI) and Th(IV) ions prior to their spectrophotometric determination. Various instrumental techniques such as elemental analysis, FTIR, and SEM analysis were employed for full characterization of the synthetic extractant. Optimization of the adsorption and elution conditions of U(VI) and Th(IV) ions using synthesized alizarin red S -impregnated XAD-2010 were studied. Langmuir isotherm model has the best fitting experimental data with a maximum adsorption capacity of 20.2 mg g^{-1} for U(VI) and 18.25 mg g^{-1} for Th(IV). The adsorption process of each metal ion by synthesized alizarin red S -impregnated XAD-2010 showed an exothermic pseudo-second-order adsorption process. The tolerance limits for several metal ions on alizarin red S -impregnated XAD-2010 were calculated, giving high tolerance limit. The optimized method was applied on international certified samples and different rock types bearing thorium and uranium with accurate results.

Keywords Separation · Spectrophotometric · Uranium · Thorium · Alizarin red S -impregnated XAD-2010

1 Introduction

The twin important nuclear elements, thorium and uranium are the corner stone of the (industrial) nuclear technology and consequently the production of nuclear fuel used in nuclear power plants which has a return on the production of huge energy capable of developing any country due to its application as an efficient fuel for electric power plants [1, 2].

Accordingly, it is a strategic issue where their exploration in their bearing rocks and hence their exploitation for production of nuclear grade yellow cake (highly concentrated uranium) is an important step in the nuclear fuel cycle. So, their accurate determination using several advanced and single techniques with economic procedures will be of great prominence for a precise and accurate evaluation of their occurrences in certain areas [3, 4].

Several instrumental techniques were suggested namely; inductively coupled plasma atomic emission spectrometry and inductively coupled plasma mass spectrometry which can serve to improve sensitivity for uranium and thorium determination where, several trials are performed to reach economic and accurate methods for their determination [5].

Problems encountering the spectrophotometric technique in rock analysis are mainly referring to spectral interference which enhances the absorbance value giving out incorrect (high) concentration [6, 7].

To solve these problems, the segregation including coprecipitation, solvent extraction, electrodeposition, ion-exchange etc. [8–10] has been used in the analytical chemistry laboratories for their precise and accurate determination. Solid phase extraction (SPE) is one of the efficient preconcentration-differentiation procedures used, due to

---

✉ Ahmed Orabi, a_orabi_chem@yahoo.com | [1]Nuclear Materials Authority, P.O. Box 530, Maadi, Cairo, Egypt. [2]Chemistry Department, Faculty of Science, Menofia University, Shibin El Kom, Egypt.

SN Applied Sciences (2019) 1:309 | https://doi.org/10.1007/s42452-019-0325-7

Received: 14 January 2019 / Accepted: 1 March 2019 / Published online: 6 March 2019

its simplicity and confined usage of the organic solvents [11–15]. Solid phase extraction of thorium and uranium is also a preferable choice in the analytical chemistry in common [16–18]. Several properties of SPE such as selectivity, simplicity of equipment, ease of operation, and the multiple usages of adsorbents for numerous separation and preconcentration cycles without deprivation in the metal ion sorption capacity have made their use popular [19–24].

Amberlite XAD resin folk are vital for solid phase extraction studies for heavy metal ions in the environmental samples [25, 26]. These resins are extremely important from both, the economic and environmental point of views for solid phase extraction after their proper functionalization [27]. The literature survey revealed that XAD-2000 and XAD-2010 are used for the preconcentration and seclusion of organic materials at trace levels; [28, 29] however, only few studies on these resins were highlighted for preconcentration of trace metals [30, 31].

Spectrophotometric method for determination (as a single cheap and available technique) using the proper sensitive and selective dye was merged with solid phase extraction technique for the solutions bearing the twin nuclear elements for a single, accurate, precise, and low cost technique for the precise determination of both elements was proposed in this work. In the pursuance of many researches on the extractant impregnated resins (EIRs) applications [21, 22, 32–37], this work converges on the eclectic separation and preconcentration of trace amounts of thorium and uranium in their bearing rocks using a new EIR containing Amberlite XAD-2010 resin beads impregnated with alizarin red S. The new EIR sorbent manifested eminent selectivity for thorium and uranium sorption from aqueous solutions after adequate optimization.

2 Experimental

2.1 Reagents

Alizarin red S (ARS) and Amberlite XAD-2010 were purchased from Sigma Chemicals. All the common reagents were supplied by VWR BDH Prolabo Chemicals (Fontenay-sous-Bois, France). On the other hand, U(VI), Th(V), Na(I), K(I), Ca(II), Mg(II), Al(III), Mn(II), Fe(III), Cr(VI), VO(II), Cu(II), Co(III), Ln(III), pb(II), Ba(II), Mo(VI), B(III), Cd(II), and Zn(II) standard stock solutions, 1000 ppm, were analytical grade and purchased from Merck (Darmstadt, Germany).

2.2 Preparation of the EIR

The ARS-impregnated XAD-2010 resin beads were prepared using dry procedure [34]. Before the impregnation process, a pretreatment of amberlite XAD-2010 resin beads were handled with 1: 1 methanol–water solution comprising 6M HCl for 12 h in order to drive out any enduring monomers and other species of impurities which may be found with the fabricated beads. The resin was totally rinsed with double-distilled water and placed into a drying oven at 323 °K for 30 min. To prepare the impregnated resin, portions of amberlite XAD-2010 resin (1 g of dry resin) were carried into a spectrum of glass stoppered bottles containing different concentrations of ARS in 200 mL methanol, which was utilized as the solvent. The entire contents were slowly shaken for 10 h to accomplish impregnation process and then were heated at 333 °K in a drying oven to drive out the solvent. Each EIR sample was then conveyed to a porous filter and washed consecutively with HCl (3M) solution and enormous amounts of distilled water until no ARS was found in the filtrate. Eventually, the impregnated resins were dried at 323 °K and weighed. Compound structure was characterized by means of SEM using a Jeol (Tokyo, Japan) JSM 5600 LV scanning electron microscope, FTIR spectrometer Bruker Vector 22 Germany in the range of 400–4000 cm^{-1}, and elemental analysis.

2.3 Analytical procedures

U and Th were spectrophotometerically determined by using the chromogenic reagent, Arsenazo-III and thoron I, respectively [38]. Other interfering elements were analyzed using ICP-OES, Teledyne technologies (Inductively Coupled Plasma Optical Emission Spectrometer).

2.4 Statistical and accuracy evaluation

Statistical techniques are applied, in the present work, in two ways: one of them is for estimating precision and accuracy of the analytical data and the second is for quality assurance of the produced concentrate. A common practice in analytical chemistry literature is to quote the mean ($\bar{X}$) as a common factor for estimating the precession (degree of reproducibility or random error). Accuracy (Δ) of a measurement method is defined as the measure of the closeness of results to reference (well known) or true one. The following equations are therefore applied [39–41]:

$$\text{Arithmetic mean: } \bar{X} = \frac{\sum X_i}{n} \tag{1}$$

where Xi, individual measurement; n, number of measurements.

$$\text{Standard deviation: } SD = \left[\frac{\sum_1^n (X_i - \bar{X})^2}{(n-1)}\right]^{1/2} \tag{2}$$

$$\text{Relative standard deviation: } RSD = SD/\bar{X} \times 100 \quad (3)$$

$$\text{Standard error: } SE = \frac{SD}{\sqrt{n}} \quad (4)$$

$$\text{The percentage error: } \%Error = SE/\bar{X} \times 100 \quad (5)$$

$$\text{Accuracy: } \Delta = \pm\sqrt{\frac{d^2}{2n}} \quad (6)$$

where d represents the difference between the repeated measurements.

2.5 Adsorption procedure

In the adsorption process, a batch technique was used to study different parameters affecting uranium and thorium adsorption process for the prepared EIR in all experiments such as pH, contact time, initial metal concentration, temperature and interfering ions. Thus, a sample (S) weight of 0.1 g (m) was added to a volume of 50 mL (*V*) of U or Th aqueous solutions and equilibrated by stirring at room temperature. After a certain time, the solutions were filtrated and the concentration of uranium and thorium was spectrophotometrically determined. Both the determination of the adsorption coefficient (Ads %) and the adsorption capacity (q) were calculated using the following equations:

$$q = \left(\frac{(C_i - C_f)}{m}\right) \times V \quad (7)$$

$$Ads\ \% = \left(\frac{(C_i - C_f)}{Ci}\right) \times 100 \quad (8)$$

where C_i and C_f are the initial and the final concentrations of aqueous phases, respectively.

3 Results and discussion

3.1 Preparation of ARS-impregnated resin

Alizarin Red S dye (ARS) contains two hydroxyl groups and sulphonate group, making it suitable for chelate formation with several metal ions. It is easily soluble in alcohol or water, and changes its colour with pH (yellow at pH < 4, orange to intense red in the pH region 4–8, and violet at pH > 9). Alizarin Red S -impregnated XAD-2010, ARS/XAD-2010, was efficiently prepared by the impregnation method, described in the experimental section. To prepare the suitable form of ARS/XAD-2010, various impregnation ratios; g ARS/g dry XAD-2010 adsorbent were studied and the data was illustrated in Fig. 1. As shown, the weight change (%) increases as the impregnation ratio increases after which a plateau is reached at the impregnation ratio of 1.5 g ARS/g dry XAD-2010 adsorbent, where it was adopted as the optimum impregnation ratio.

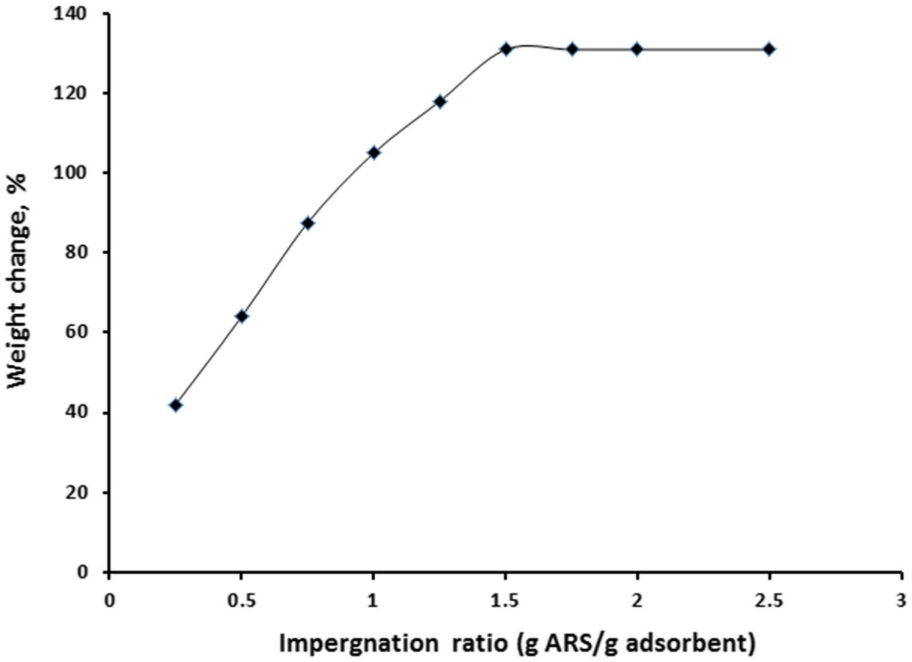

Fig. 1 Effect of the impregnation ratio on the EIR preparation at the condition that portions of 1-g of the dry polymer beads of Amberlite XAD-2010 was subjected to the impregnation process

3.2 Stabilizing extractant capacity impregnated on the polymer

The immobilization of the extractant on the macroporous matrices during the impregnation process is invaded in pores (due to the capillary forces) and in the gel regions of the polymer beads. The impregnated extractant located in pores is weakly bonded and represents the unstable part of EIR capacity; thus, it can be easily leached out from the freshly prepared EIR sample. Otherwise, the most stable part and remains constant that is taken up by the gel regions of the macroporous matrix [42, 43]. According to Hosseini-Bandegharaei et al. [44], the chemical stability of the Extractant Impregnating Resin (ARS/XAD-2010) was examined by sequentially suspending a 0.1 g of EIR in different pH values and shaking for 10 h. The new EIR was filtered and rinsed with double distilled water; the resulted solution was clear. The released amount of ARS was examined by weighing the EIR (ARS/XAD-2010). It was found that no change in its quantity indicates a high stability.

3.3 Characterization of the modified resin

In order to verify the presence of the active functional groups of ARS in the modified resin, IR spectra of Amberlite XAD-2010 and the ARS/XAD-2010 modified resin were obtained (Fig. 2). The IR spectrum of amberlite XAD 2010 resin exhibited less intense band at 3436 cm^{-1}, which can be attributed to the stretching vibrations of adsorbed water [45]. The bands at 2924 and 1632 cm^{-1} are assigned to the aliphatic –CH_2–CH_2 chains and the phenyl rings, respectively [46–49].

Upon modification with ARS, the phenolic-OH band appears at 3432 cm^{-1} [46, 50]. The most noticeable change in the spectra is the band at 1266 and 1159 cm^{-1} which are due to the stretching SO_3^{2-} and C–S band at 585 cm^{-1} [46, 51]. The band at 1022 cm^{-1} is assigned to the stretching vibration of S=O group. Moreover the bands were assigned to C–O at 1061 and 1105 cm^{-1} and the C=O band at 1635 cm^{-1} [46, 48, 49, 51–53]. The above mentioned bands indicate the modification of amberlite XAD 2010 with ARS.

The CHNS elemental analysis of Amberlite XAD-2010 and the ARS/XAD-2010 modified resin were obtained (Table 1). The elemental analysis of the ARS/XAD-2010 was conducted with an erratic increase in the C, H and N contents than Amberlite XAD-2010. In addition, the presence of S element (3.15%) confirms the impregnation of ARS into Amberlite XAD-2010 as shown in Table 1.

Table 1 The CHNS elemental analysis of Amberlite XAD-2010 and the ARS/XAD-2010 modified resin

Sample	C	H	N	S
Amberlite XAD-2010	39.12	5.03	3.26	–
ARS/XAD-2010 modified resin	64.63	6.45	3.73	3.15

Fig. 2 FTIR spectroscopy of the working polymeric resin: (A) Amberlite XAD-2010 and (B) ARS/XAD-2010 modified resin

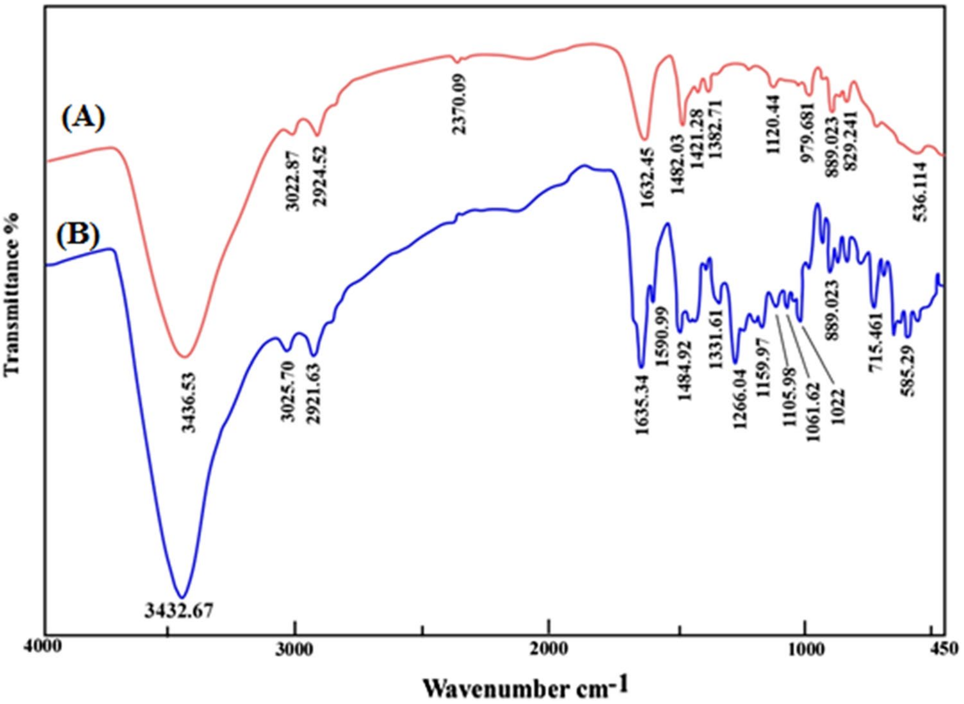

3.4 Effect of acid medium

From the critical parameters for solid phase extraction of metal ions is the type of acidic medium. The effect of perchloric acid, hydrochloric acid, nitric acid and sulfuric acid on sorption process and complex formation between metal ions and synthesized EIR were studied. For this purpose, 50 mL aliquots of U(VI) and Th(IV) solutions (pH 3) having concentration of 500 μg L^{-1} in different acid concentrations were treated with 0.1 g portions of EIR at 298 ± 1 K. As shown in Table 2, the adsorption of metal ions on synthesized EIR with perchloric acid gives the highest adsorption percentages. As expected, increasing acid concentration leads to enhance the salt effect and consequently, the adsorption process is encountered with some restriction. Also, the crystals of salt occupy the superficial area of the EIR at high salt concentrations, which diminish the EIR available to interact with the analytes and play a very negative role by decreasing the recovery. The same behavior agrees with that reported earlier using other adsorbents [22, 44, 54, 55]. Perchloric acid was selected for optimum adsorption experiments.

3.5 Effect of pH

As mentioned above, the synthesized EIR (ARS/XAD-2010) can take up uranium and thorium in high yield from aqueous perchloric acid solutions containing uranium and thorium. A glance at the extractant structure shows the presence of different donating atoms or functional groups such as OH, C=O, and S-donor ligands which readily form complexes with uranium and thorium ions. The pH extensively affects the metals ion accumulation on the sorbent and their chelate formation. The effect of pH on the adsorption process was investigated in the range of 1–5 under the above optimum conditions (Fig. 3).

It was found that the adsorption of uranium was very low at perchloric solution (0.01 M) with lower pH value but, thorium can be adsorbed effectively with 98% yield and then declines slowly to 20% solution at pH 5 by synthesized EIR (ARS/XAD-2010) due to the formation of thorium hydroxide precipitate species after pH 3.5 [56, 57]. On the other hand, uranium gives high yield of adsorption at pH 4 and begins to decrease above pH 4.5, due to the formation of colloidal and oligomeric species that can precipitate uranium as hydroxides in the solution or at the surface of the sorbent [56–59]. The result agreed with that reported earlier using other adsorbents [22, 54, 55]. Lower adsorption of each analyte at pH values lower

Table 2 The effect of different acid concentrations of several acidic media

Acid conc.	Th adsorption (%)				U adsorption (%)			
	$HClO_4$	HNO_3	HCl	H_2SO_4	$HClO_4$	HNO_3	HCl	H_2SO_4
0.01	75.0	62.5	70.0	50.0	78.0	60.0	66.0	54.0
0.025	70.0	54.0	56.0	40.7	66.0	50.0	52.0	43.0
0.05	50.0	43.0	43.2	30.4	48.2	40.0	45.8	32.3
0.10	42.0	31.4	33.5	25.6	38.2	31.6	36.8	24.8

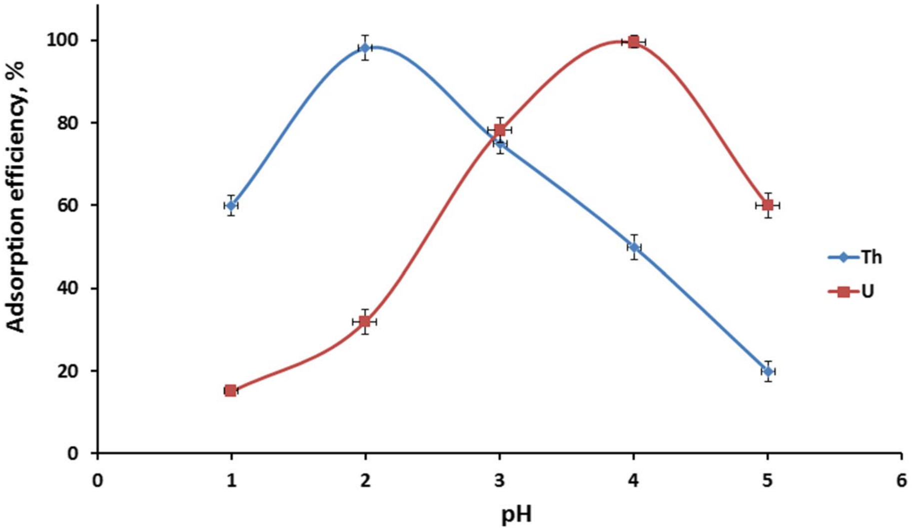

Fig. 3 Effect of pH on the adsorption efficiency percent of uranium and thorium using 50 mL of solution of 0.5 mg L^{-1} with respect to U(VI) and Th(IV) ions and 10 min contact time

than the optimum values can be due to (1) the rivalry of H^+ with analyte ions for special functional groups, which are responsible for complexation of each analyte to ARS/XAD-2010, (2) partial protonation of the functional groups of extractant molecules. So, the adsorption of the analyte thorium ion was quite high and comparable suggesting marginal or no interference from uranium at lower pH (2). As a result of the above, the authors suggested separation of thorium firstly by the synthesized EIR (ARS/XAD-2010) from perchloric solution then effluent was subjected to uranium adsorption with a high yield of selectivity.

3.6 Effect of contact time and kinetic studies

Kinetic behavior of uranium and thorium adsorption from 0.01 M perchloric acid solution using the synthetic sorbent, in terms of adsorbed amount q_t (mg g^{-1}), is illustrated in Fig. 4. The adsorption into synthesized EIR (ARS/XAD-2010) is passed through two stages:, the first stage where adsorption increased rapidly up to 5 min which is attributed to more available sites of EIR for adsorption, and finally equilibrium stage has been attained at 10 min (Fig. 4) referred to all the sites present on adsorbent get satisfied [60, 61]. It can be seen that over 75% of uranium and thorium adsorption efficiency achieved within the first 3 min. In addition, equilibrium adsorption (99.2% for U and 98% for Th) occurred within 10 min.

The experimental data was treated with various kinetic models including the pseudo-first order and the pseudo-second order for evaluating the kinetic mechanism of adsorption process.

The equations of pseudo-first-order and pseudo-second-order models are specified as follows [62, 63]:

$$\log(q_e - q_t) = \log\ q_e - \frac{k_1 t}{2.303} \tag{9}$$

$$\frac{t}{q_t} = \frac{1}{k_2 q_e^2} + \frac{t}{q_e} \tag{10}$$

where q_e and q_t (mg g^{-1}) are the capacities of each analyte adsorption by synthesized EIR at equilibrium and time t respectively. k_1 (1/min) and k_2 (g mg^{-1} min^{-1}) is pseudo first-order and second order sorption rate constants respectively. The values of constants (q_e, k_1, and K_2) were calculated from the lines (Fig. 5) and given in Table 3. Consequently, Pseudo second order model has better fitting experimental data performance in terms of higher correlation coefficient and conformity with equilibrium adsorbed amount *qe*.

The intra-particle diffusion model is expressed as [64, 65]:

$$q_t = k_{id} t^{0.5} + C \tag{11}$$

where q_t (mg g^{-1}) is the metal adsorbed amount at time t, K_{id} (mg g^{-1} $min^{0.5}$) is the intraparticle diffusion rate constant and C is the thickness of the boundary layer.

The intraparticle diffusion parameters are calculated from the slope and the intercept of the linear plots as expressed in Fig. 6. The plots of q_t versus $t^{0.5}$ show that the obtained straight lines do not pass through the origin ($C > 0$). The obtained data in Table 3 is found that the values of correlation coefficient R^2 are 0.94 and 0.96 for Th and U respectively. The obtained data confirm that this model is not appropriate for describing the sorption kinetics. Finally, from the kinetic parameters of three kinetic models as seen in Table 3, the adsorption kinetics

Fig. 4 Effect of time upon uranium and thorium adsorption efficiency from 50 mL 0.01 M perchlorate medium ((500 µg L^{-1} of each U and Th) by 0.1 g synthesized EIR at 25 °C

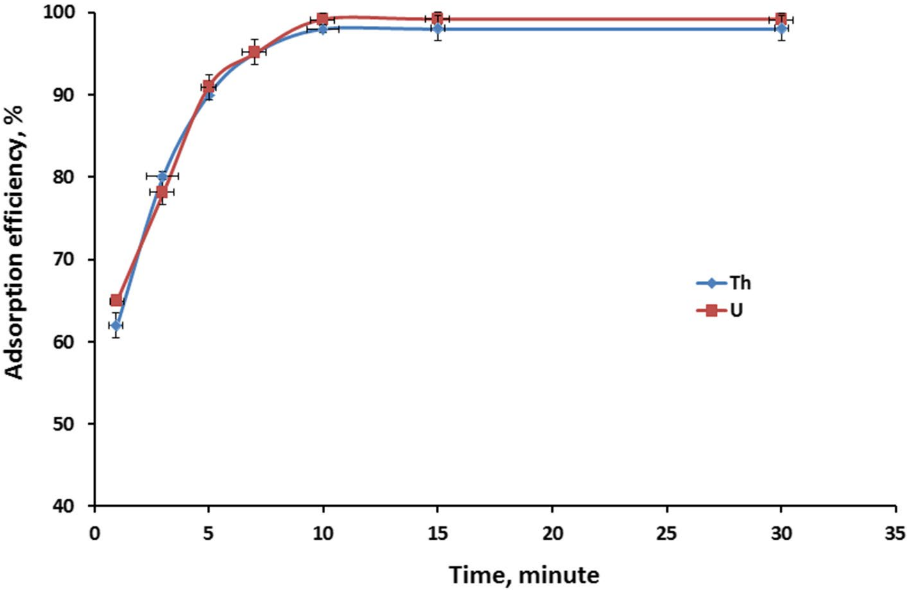

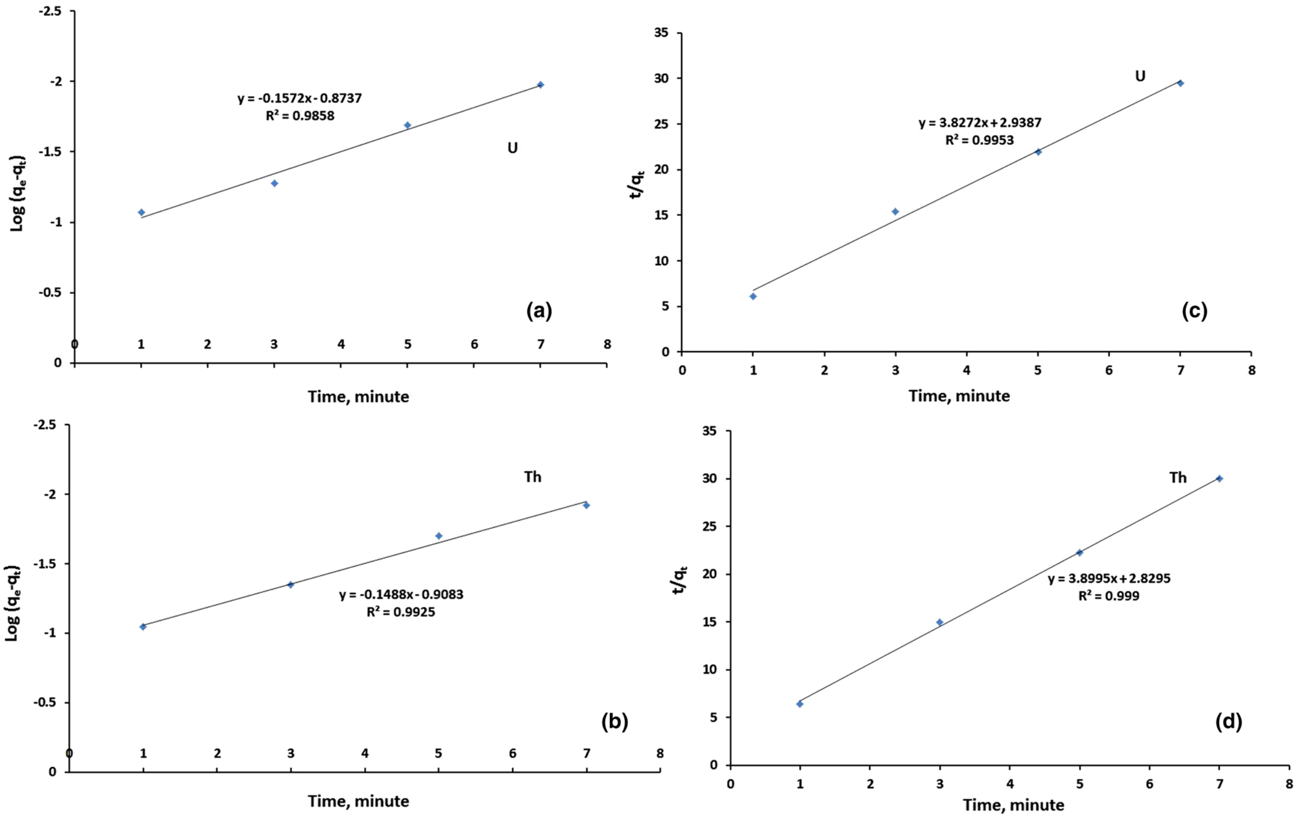

Fig. 5 Pseudo-first-order (**a**, **b**) and pseudo-second (**c**, **d**) kinetics of U and Th adsorption by synthesized EIR from the synthetic perchloric acid (0.01 M $HClO_4$ and 0.5 mg L^{-1} of each U and Th) at 25 °C

Table 3 Kinetic parameters for the adsorption of U(VI) and Th(IV) ions onto synthesized EIR (ARS/XAD-2010)

Metal ions	Exp. q_e (mg g^{-1})	Pseudo-First-order			Pseudo-Second-order			Intraparticle diffusion		
		q_e (mg g^{-1})	K_1 (min^{-1})	R^2	q_e (mg g^{-1})	K_2 (g mg^{-1} min^{-1})	R^2	k_{id} (mg g^{-1} $min^{-1/2}$)	C (mg g^{-1})	R^2
U(VI)	0.248	0.134	0.362	0.985	0.261	5.00	0.995	0.0402	0.1219	0.96
Th(IV)	0.245	0.124	0.343	0.992	0.256	5.37	0.999	0.0416	0.1266	0.94

is estimated and fitted well by the pseudosecond-order kinetic model.

3.7 Effect of initial U and Th concentration and the adsorption mechanism

Based on mixing a series of batch experiments at ambient temperature (≈ 25 °C), it can be concluded that the adsorbed uranium and thorium increases with increasing the initial uranium and thorium concentrations in solution till the saturation plateau. The maximum uranium and thorium sorption capacity was acquired by conducting a fixed EIR (ARS/XAD-2010) weight (0.1 g) with 50 mL of U and Th at different concentrations in perchloric acid (0.01 M), and at optimum conditions for each metal ion. From Fig. 7, we can conclude that the maximum adsorption capacity of uranium and thorium from perchloric acid by EIR (ARS/XAD-2010) was 19 mg U g^{-1} EIR and 17 mg Th g^{-1} EIR. It is interesting to compare the achieved U(VI) and Th(IV) adsorption capacities on the synthesized EIR with other previously prepared sorbents. It was found that the synthesized EIR is competitive when compared with other previously prepared sorbents such as Mannich type resin (*q*max: 5.2 mg U g^{-1} and 2.28 mg Th g^{-1} [57]), modified benzophenone (qmax: 2.42 mg U g^{-1} [66] and 1.1 mg Th g^{-1} [67]), Carminic acid (CA) impregnated XAD-16 (1.93 mg U g^{-1} and 1.92 mg Th g^{-1} [22]), Quinoline-8-ol impregnated XAD-4 (qmax: 2.74 mg U g^{-1} [68]), o-Vaniline semicarbazone impregnated XAD-4 (qmax: 2.89 U g^{-1} [69], Pyrogallol impregnated XAD-2 (qmax: 6.71 mg U g^{-1} [70]),

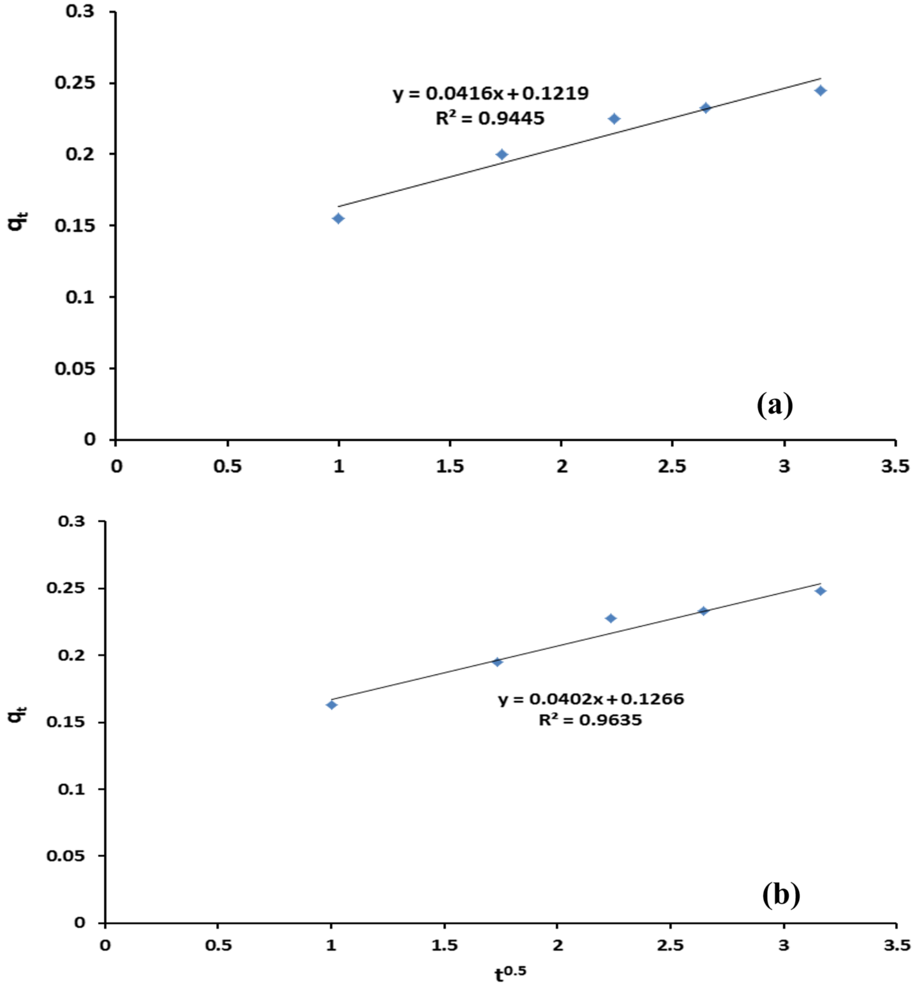

Fig. 6 Intra-particle diffusion model of Th(IV) (**a**) and U(VI) (**b**) adsorption by 0.1 g synthesized EIR from 50 mL 0.01 M perchloric acid (500 μg L^{-1} of each U and Th) at 25 °C

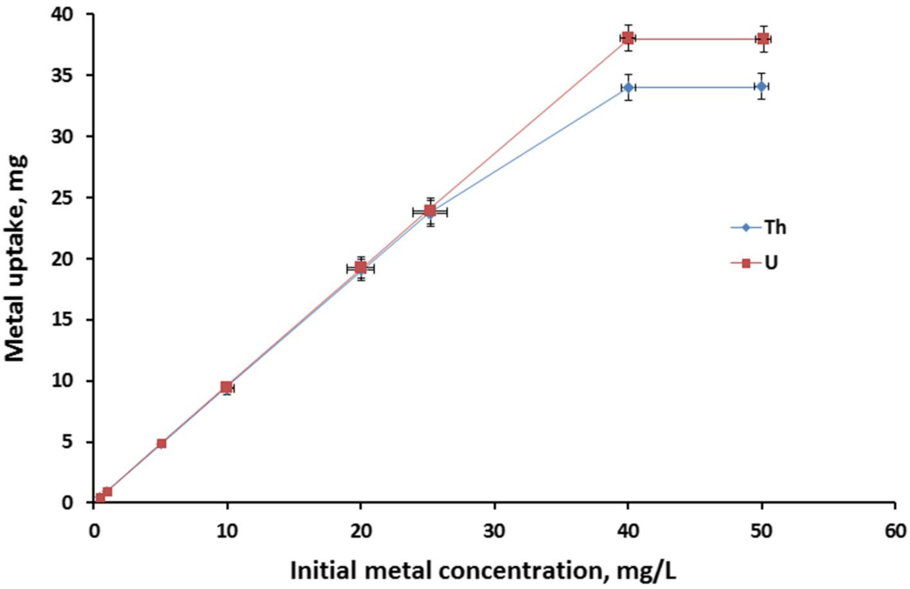

Fig. 7 Effect of initial uranium and thorium concentrations on adsorption efficiency of synthesized EIR from perchlorate medium (adsorption condition: 50 mL of solution of 0.01 M perchloric acid and 10 min contact time at room temperature)

modified naphthalene (qmax: 1.88 mg U g^{-1} [20]), modified silica (qmax: 3.02 mg U g^{-1} [71]), Tiron impregnated XAD-2 (qmax: 7.70 mg U g^{-1} [72]), and [(2-dihydroxyarsinoylphenylamino) methyl] phosphonic acid functionalized XAD-16 (3.55 mg U g^{-1} and 3.25 mg Th g^{-1} [73]).

The infrared technique was used for further study of the adsorption mechanism (Fig. 8). Comparing both spectra of EIR before and after adsorption, it can be observed that the main difference between absence of thorium and uranium ions (Fig. 2B) and their complexation with synthesized resin (Fig. 8A, B) was some band shifts which were observed due to interaction with U and Th. The band belonging to C=O unit of synthesized resin shifted to 1637 cm^{-1}. Also, the IR spectrum of the modified resin loaded with uranium and thorium is also characterized by the shift of C–O bands to 1234, 1188, 1161, and 1090 cm^{-1}. The band of OH becomes weak and less intense due to the interaction with U and Th ions. As a result, we can say that the ketonic and phenolic groups are coordinated to the U and Th ions and the result agreed with that reported earlier [22, 46, 50, 74, 75] which indicate that sorption of uranium and thorium takes place through complexation with ARS loaded on the resin and that amberlite XAD 2010 is applied only as an immobilization substrate for ARS reagent.

From the SEM images of the ARS/XAD-2010 synthesized resin before and after uranium(VI) and thorium(IV) adsorption are shown in Fig. 9a–c, respectively. The SEM images show the observation of brilliant spots on the resin beads variation after U(VI) and Th(IV) adsorption other than that uniformity and smooth surface of ARS/XAD-2010 synthesized resin.

As could be seen from the results, a visible change of the surface morphology in the U(VI) and Th(IV) adsorbed resin demonstrates that the sorption of studied metal ions take place onto the ARS/XAD-2010 synthesized resin.

3.8 Isotherm studies

In order to describe and understand the adsorption properties of uranium and thorium from 0.01 M perchloric acid towards synthesized EIR, Langmuir and Freundlich models were established to fit the experimental data. The equation of Langmuir (12) and Freundlich (13) models are specified as follows [76]:

$$\frac{C_e}{q_e} = \frac{C_e}{q_{\max}} + \frac{1}{K_L q_{\max}} \tag{12}$$

$$\log\ q_e = \log\ K_f + \frac{\log\ C_e}{n} \tag{13}$$

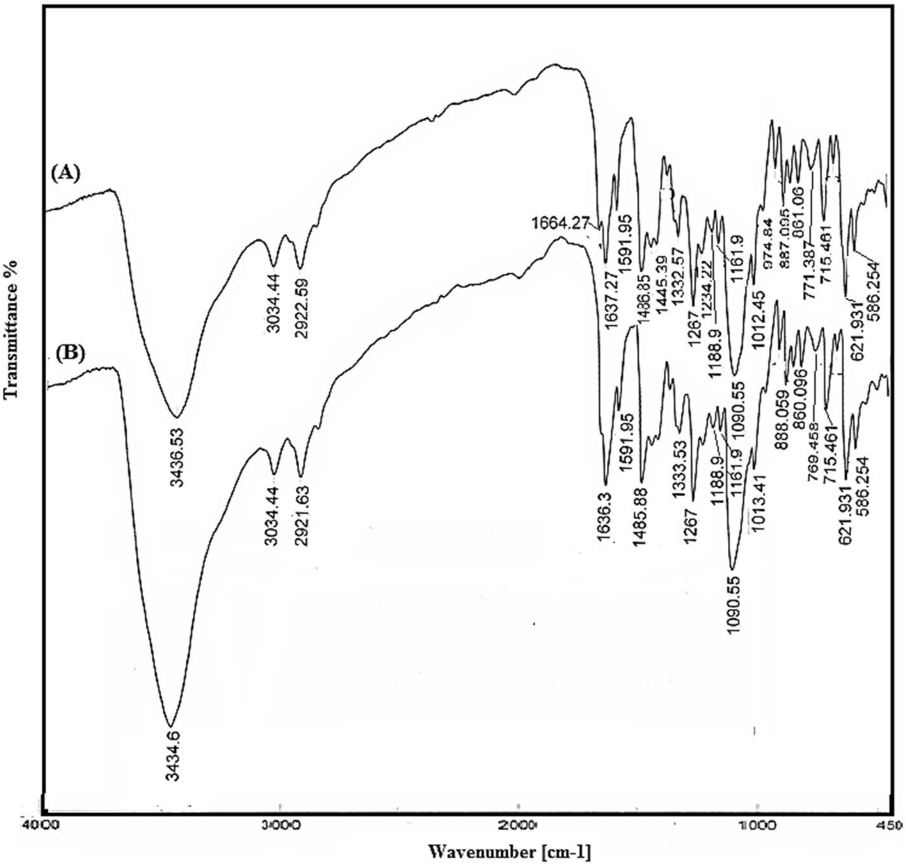

Fig. 8 FTIR spectroscopy of Th-loaded synthesized (ARS/XAD-2010) (A) and U-loaded synthesized (ARS/XAD-2010) (B)

Fig. 9 SEM images of ARS/XAD-2010 (**a**), U-loaded ARS/XAD-2010 (**b**) and Th- loaded ARS/XAD-2010 (**c**)

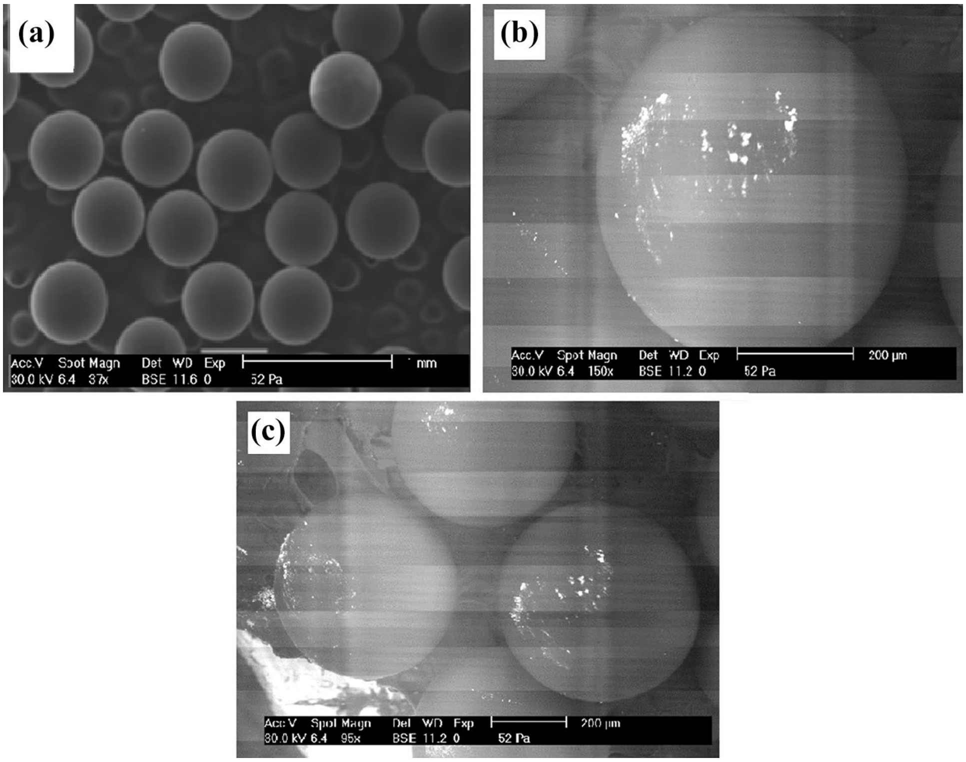

Here *Ce* (mg L^{-1}) is the equilibrium concentration of metal in the liquid phase, q_{max} (mg g^{-1}) is the monolayer capacity in model of langmuir, K_L (L mg^{-1}) is the Langmuir equilibrium constant, k_f and *n* are characteristic Freundlich constants related to the relative sorption capacity of the sorbent and sorption intensity, respectively.

The linear plots of (C_e/q_e) versus C_e for Langmuir isotherm (Fig. 10a, b) or log q_e versus *log* C_e for Freundlich isotherm (Fig. 10c, d) give the constants of these models, from slope and intercept, which are given in Table 4 and represented adsorption properties of uranium and thorium from 0.01 M perchloric acid towards synthesized EIR. Consequently, Langmuir isotherm model has better fitting experimental data performance in terms of higher correlation coefficient and conformity with equilibrium uranium and thorium adsorbed amount from perchlorate medium.

Dubinin–Radushkevich (D–R) does not assume an energetically homogeneous surface and proposes a non-homogenous distribution of adsorption sites. In particular, it assumes that the ionic species bind first with the most energetically favorable sites and that multilayer adsorption then occurs. The linear form of D–R isotherm equation [77, 78]:

$$\ln\ q_e = \ln\ q_m - k\varepsilon^2 \tag{14}$$

where q_m is the theoretical saturation capacity (mg g^{-1}), K (mol^2 KJ^2) is a constant related to the mean free energy of adsorption per mole of the adsorbate, ε is the Polanyi potential ($\varepsilon = RT\ \ln\ (1 + 1/Ce)$), Ce is the equilibrium concentration of adsorbate in solution, R (8.314 J mol^{-1} K^{-1}) is the gas constant, and T is the absolute temperature. The D–R constants q_m and K are calculated from the linear plots of ln q_e versus ε^2 from the intercept and slope (Fig. 11). The constant K gives an idea about the mean free energy (E) of adsorption per molecule of the adsorbate when it is transferred to the surface of the solid from infinity in the solution and can be calculated from the relationship [77]:

$$E = \frac{1}{\sqrt{2K}} \tag{15}$$

If the magnitude of E is between 8 and 16 kJ mol^{-1}, the sorption process is supposed to proceed via chemisorption but if E is less than 8 kJ mol^{-1}, the sorption process is of physical nature [79, 80].

E for uranyl and thorium ions is 0.173 and 0.2 kJ mol^{-1} respectively (less than 1) implying that U(VI) and Th(IV) adsorption process proceeds via physisorption and the values of correlation coefficient (R^2) are 0.85 and 0.86 at 298 K, respectively. Therefore, the Dubinin–Radushkevich (D–R) isotherm model does not fit the adsorption processes of the uranium and thorium ions on the synthesized EIR. Finally, it is clear from Table 4 and Figs. 10 and 11 that the parameters of Langmuir isotherm model are closer to the experimental values than those fitted by other models.

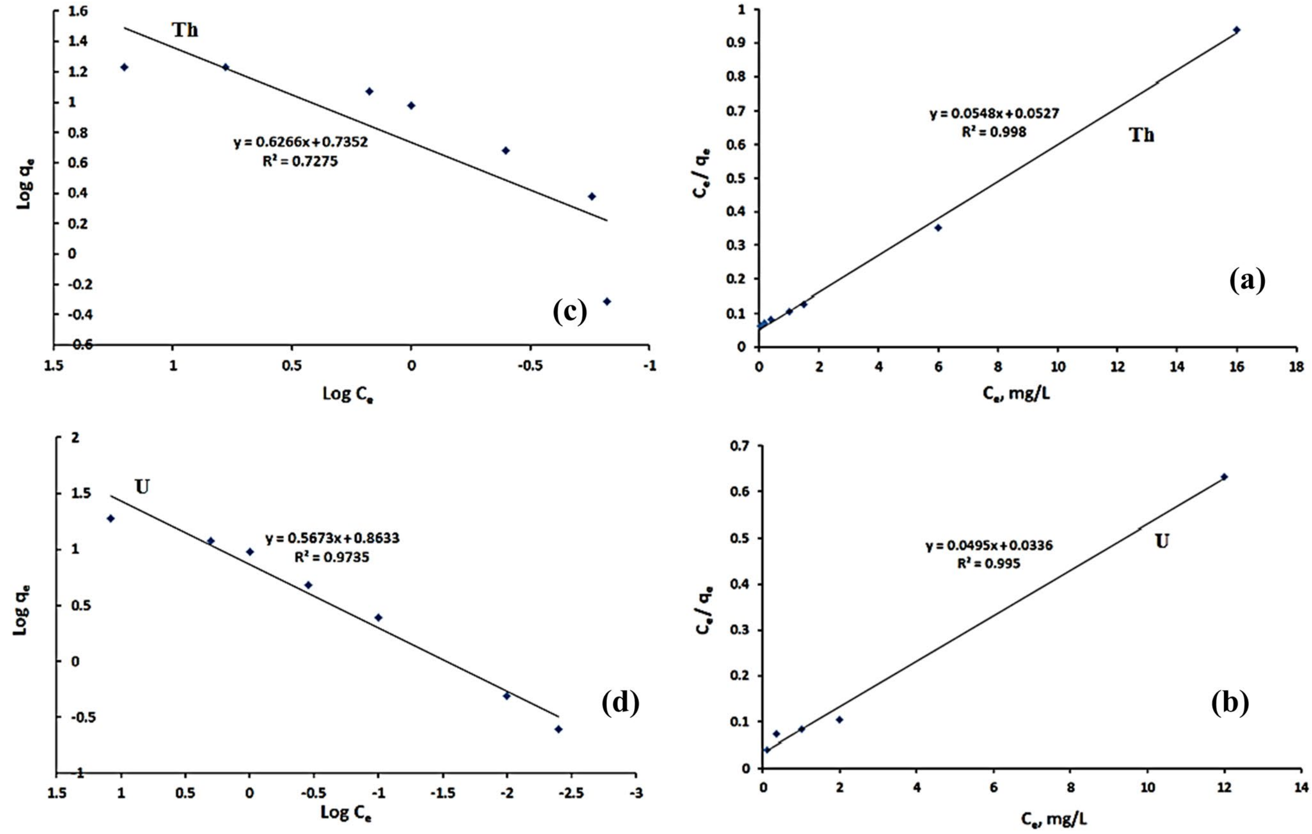

Fig. 10 Langmuir (**a**, **b**) and Freundlich (**c**, **d**) models of U and Th adsorption by synthesized EIR (Adsorption condition: 0.1 g EIR, 50 mL of solution of 0.01 M perchloric acid, 10 min contact time at 25 °C)

Table 4 Isotherm parameters for the adsorption of U(VI) and Th(IV) ions onto synthesized EIR (ARS/XAD-2010)

Metal ions	Exp. q_{max} (mg g^{-1})	Langmuir parameters			Freundlich parameters		
		q_{max} (mg g^{-1})	K_L (L mg^{-1})	R^2	n	K_f (mg g^{-1})	R^2
U(VI)	19	20.20	1.47	0.995	1.76	7.30	0.973
Th(IV)	17	18.25	1.04	0.998	1.59	5.44	0.727

These showed that Langmuir isotherm model could well describe the adsorption equilibrium of uranium and thorium ions on the resin.

3.9 Effect of temperature (thermodynamics studies)

For evaluation of the effect of temperature on adsorption of U(VI) and Th(IV) from perchloric acid (0.01 M) using synthesized EIR (ARS/XAD-2010), the adsorption process was conducted in a series of batch experiments under various temperatures ranging from 25 to 65 °C. The other parameters were as follows: concentration of each uranium and thorium 0.5 mg L^{-1}, EIR amount 0.1 g, solution volume 50 mL. As seen from Fig. 12, heating in the examined range only slightly affects the adsorption. Therefore, 25 °C can be considered as the optimum temperature for uranium adsorption experiments.

According to Lima et al. 2019 [81], the accurate estimation of thermodynamic parameters for adsorption system needs a correct equilibrium thermodynamic constant (K_e^0) to be used in Van't Hoof equation. So, it is necessary to obtain the isotherms of adsorption at several temperatures and for the best isotherm model obtain the equilibrium constant ($K_{isotherm}$). Then, this $K_{isotherm}$ should have their value converted from L mg^{-1} into L mol^{-1}. In that situation, the best isotherm model that was adjusted to the equilibrium data was the Langmuir model. Therefore, the k_L (L mol^{-1}) was used in the Van't Hoof equation, in order to estimate the thermodynamic parameters (ΔH, ΔS, and ΔG) [81]:

$$K_e^0 = K_L/\gamma \quad (16)$$

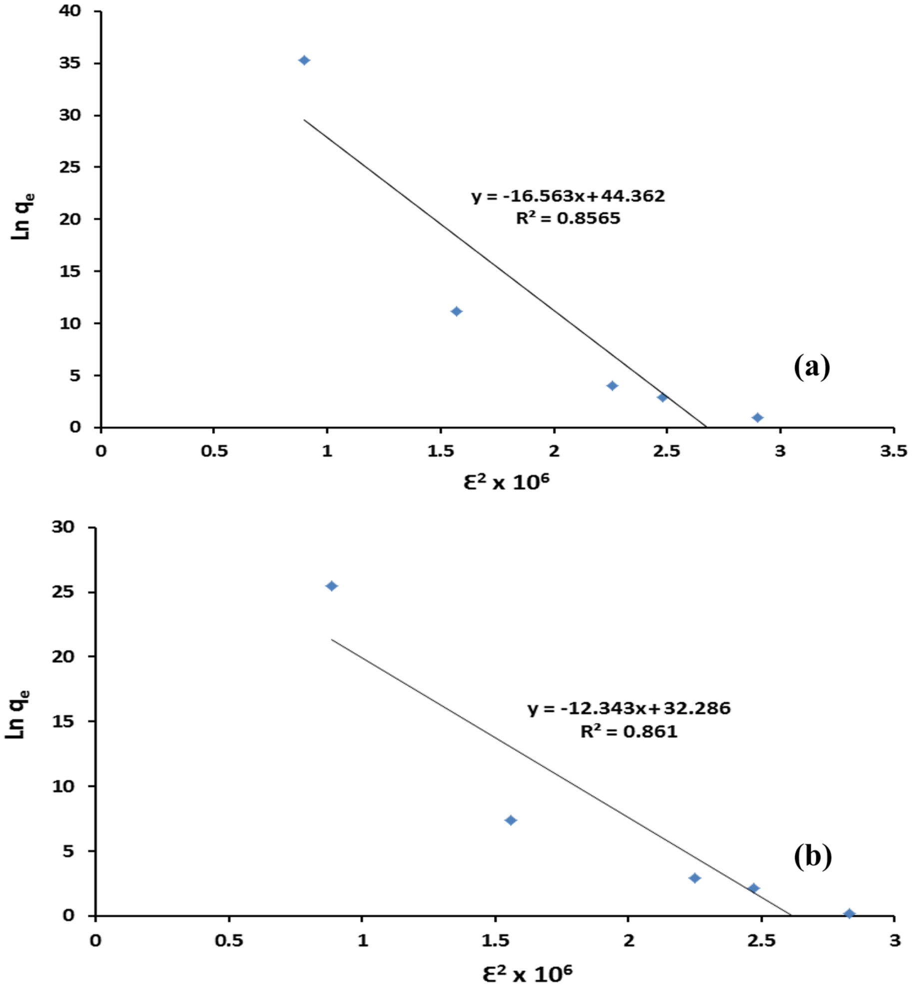

Fig. 11 The Dubinin–Radushkevich (D–R) isotherm model of uranium (**a**) and thorium (**b**) adsorption on synthesized EIR (Adsorption condition: 0.1 g EIR, 50 mL of solution of 0.01 M perchloric acid, 10 min contact time at 25 °C)

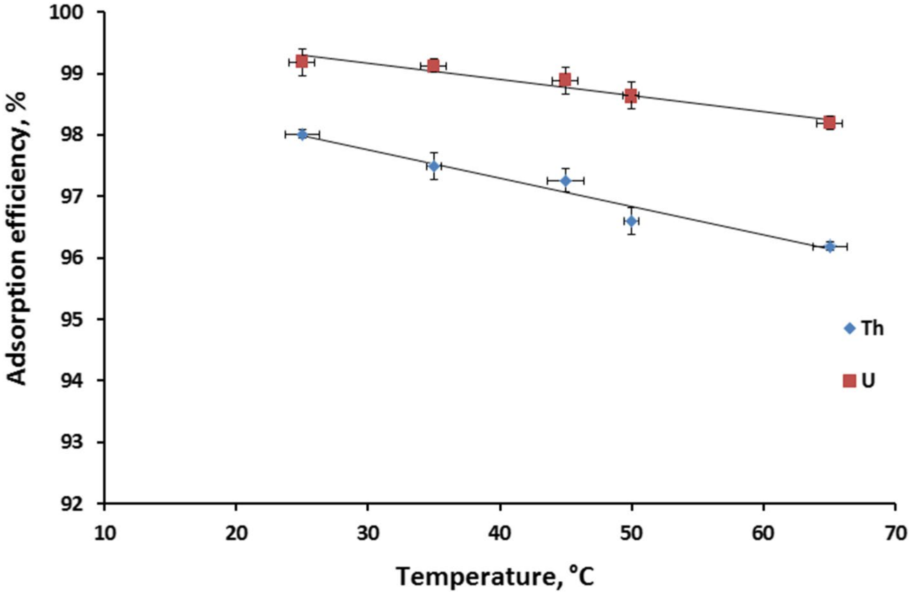

Fig. 12 Effect of temperature on the adsorption efficiency of uranium and thorium using synthesized EIR (ARS/XAD-2010) adsorbent (adsorption condition: 50 mL 0.5 mg L^{-1} of each uranium (pH 4) and thorium (pH 2) ions solution, 0.01 M perchloric acid, 0.1 g EIR, 10 min contact time)

$$\ln\left(K_e^0\right) = -\Delta H/RT + \Delta S/R \quad (17)$$

$$\Delta G = \Delta H - T\Delta S \quad (18)$$

where K_e^0 (L mol^{-1}) is the thermodynamic equilibrium constant, γ is the coefficient of activity, and the slope and intercept of the linear relation between ln K_e^0 and T^{-1} (Fig. 13) were used for calculation of enthalpy (Δ*H*, kJ mol^{-1}) and entropy (Δ*S*, J mol^{-1} K^{-1}) respectively. The negative value of ΔH (– 9.43 kJ mol^{-1} for U and – 10.27 kJ mol^{-1} for Th) indicated that the adsorption process of U(VI) and Th(IV) by EIR was an exothermic reaction. The values of ΔS are 75.95 J mol^{-1} K^{-1} for U and 69.23 J mol^{-1} K^{-1} for Th. Negative Gibbs free energy Δ*G* value (– 32.06 kJ mol^{-1} for U and – 30.9 kJ mol^{-1} for Th) demonstrated the spontaneous property of this adsorption [82–84].

3.10 Interference effect

Studying the interference effect was necessary for spectrophotometric determination of thorium and uranium in different geological rock samples. Some of the common cations which are associated with studied metals and may show sorption behavior on the ARS-modified resin interferes during their spectrophotometric determination namely, Na^+, K^+, Ca^{2+}, Mg^{2+}, Al^{3+}, Mn^{2+}, Fe^{3+}, Cr^{6+}, VO^{2+}, Cu^{2+}, Co^{3+}, Sr^{2+}, and Ln^{3+}.

In the present experimental section, the effects of the above listed cations were studied by adding different volumes from their working solutions to a constant concentration of each uranium and thorium (1 µg mL^{-1}). The absorbances of these mixtures were measured in aqueous solutions after contacting with ARS/XAD-2010 adsorbent at the optimized conditions. From the obtained results (Table 5), it was found that;

1. The alkaline earth metals did not interfere on the preconcentration process.
2. The cations such as Cu^{2+}, Zn^{2+}, Fe^{3+}, Co^{3+}, Pb^{2+} and Cd^{2+}, start to show their significant interference at concentration limits above 500 and 200 times greater than this of Th and U respectively.
3. The cations such as VO^{2+}, Ni^{2+} and Ln^{3+} start to show their significant interference at concentrations 100 times greater than this of U and 300, 250, 500 respectively times greater than this of Th.

Table 5 Effect of foreign ions on the adsorption of uranium and thorium from perchlorate solution with equal concentration of 1 µg mL^{-1} for both analytes

Interfering ion	Tolerance ratio	
	Th(IV)	U(VI)
Ca^{2+}	5000	1000
Mg^{2+}	5000	1000
Na^+	5000	1000
K^+	5000	1000
Sr^{2+}	5000	1000
Al^{3+}	5000	1000
Mn^{2+}	5000	1000
Fe^{3+}	500	1000
Co^{2+}	500	200
Cu^{2+}	500	200
Zn^{2+}	500	200
Cd^{2+}	500	200
VO^{2+}	300	100
Ni^{2+}	250	100
Pb^{2+}	500	200
Ln^{3+}	500	100

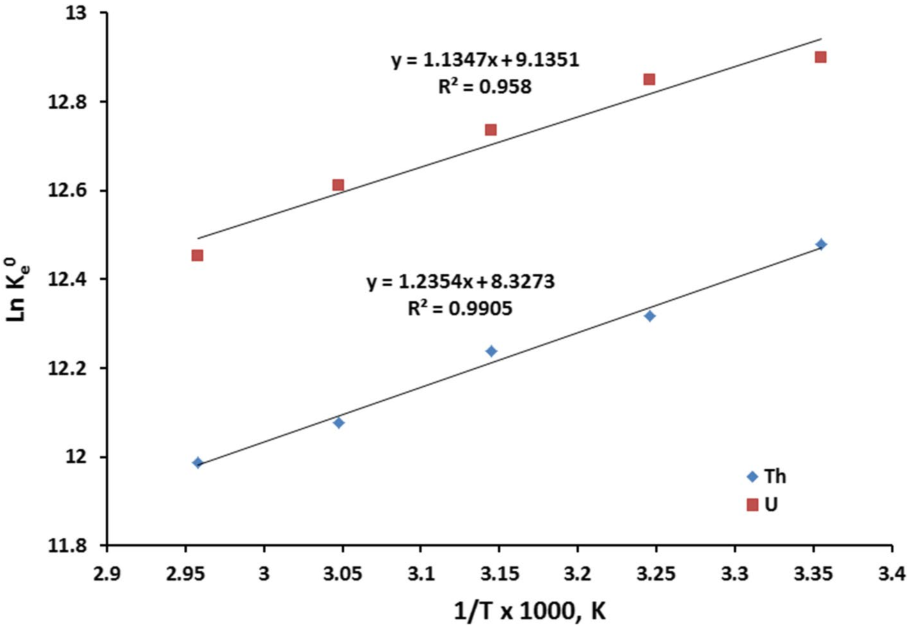

Fig. 13 The plot of Ln K_d versus 1/T of the uranium and thorium adsorption upon synthesized EIR (Adsorption condition: 0.1 g EIR, 50 mL 0.5 mg L^{-1} of each uranium (pH 4) and thorium (pH 2) ions solution, 0.01 M perchloric acid, 0.1 g EIR, 10 min contact time, at 25 °C)

3.11 Elution studies

Quantitative desorption of U(VI) and Th(IV) was performed with various eluting agents such as hydrochloric acid, ammonium oxalate, ammonium carbonate, and nitric acid which form stable complexes with uranium and thorium [22, 55, 57, 84, 85]. For this purpose, 10 mL aliquots of each eluting agent (1 M) were treated with 0.1 g portions of loaded EIR at 298 ± 1 K for 10 min. The elution of metal ions with ammonium oxalate was 56% for Th and 30% for U. The elution with ammonium carbonate was 6% for Th and 68% for U. while with hydrochloric and nitric acid, it was 99.4–32.5% for Th and 99.6–43.4% for U respectively. Hydrochloric acid was selected for optimum elution experiments.

3.12 EIR reusability

The EIR reusability was checked by subjecting the synthesized EIR (ARS/XAD-2010) to several loading and elution experiments. The capacity of the synthesized EIR (ARS/XAD-2010) was found to be practically constant (variation < 1%) after its repeated use for more than 40 runs, thus indicating the multiple use of EIR is feasible.

3.13 Application of proposed method for standard geological and granitic samples

The proposed method was applied for preconcentration and determination of U(VI) and Th(IV) in different samples including reference and geological materials to verify applications and validations of it. The samples were firstly decomposed by Afifi et al. and Fouad et al. [86, 87] to overcome the high concentration of major oxides. The serious interference from above studied cations was avoided by masking with potassium cyanide (1×10^{-3} M) [88], Then, uranium and thorium was separated from acidic solution using synthesized EIR (ARS/XAD-2010) adsorbent at optimum conditions and analyzed in the eluted solutions spectrophotometrically with good accuracy (Tables 6, 7). Thus, these results indicated that the proposed method is accurate, simple and cost-effective for analyzing ore samples containing uranium and thorium.

4 Summary and conclusions

A combination between spectrophotometric procedure and separation of U(VI) and Th(IV) ions by a high stable EIR is described. The new EIR was prepared by impregnating alizarin red S onto Amberlite XAD-2010 beads. The maximum sorption capacity respect to interested

Table 6 Comparison of uranium and thorium concentrations in standard reference rock samples and found using present method

Standard sample	Certified value (ppm)	Concentration of U, Th found using present method (ppm)	SD	SE	Error %	Accuracy
DL-1a[a]	76 Th	75.3	0.57	0.33	0.44	± 0.64
		75.5				
		76.6				
	116 U	115.2	0.89	0.51	0.44	± 0.88
		115.6				
		116.9				
DH-1a[a]	91Th	90.3	0.62	0.36	0.39	± 0.62
		90.6				
		91.5				
	2629 U	2627.5	1.05	0.61	0.023	± 0.95
		2625.6				
		2626.7				
Nim.G[b]	51 Th	50.6	0.73	0.42	0.83	± 0.62
		51.5				
		50.3				
	15 U	15.5	0.36	0.21	1.33	± 0.36
		15.3				
		16.0				

[a] Certified values reported by Canadian Central for Mineral and Energy Technology standards (CANMET), certifying agency. *SD* standard deviation, *SE* standard error

[b] Certified values reported by SA Bureau of standards P/Bag X191, Pretoria 0001 (SARM1)

Table 7 Comparison between uranium and thorium concentrations in the granitic rock samples using the present method

Granitic sample ID	Expected U, Th concentration (ppm)	Concentration of U, Th found using present method (ppm)	SD	SE	Error %	Accuracy
M40	412 Th	413.0	0.60	0.35	0.08	± 0.40
		411.2				
		412.5				
	40 U	40.6	0.57	0.33	0.81	± 0.15
		41.4				
		40.3				
M50	160.2 Th	161.0	0.70	0.40	0.25	± 0.15
		159.7				
		159.9				
	50 U	51.5	0.73	0.42	0.83	± 0.624
		50.6				
		50.3				
M53	290.5 Th	289.2	0.35	0.20	0.07	± 0.35
		288.9				
		288.5				
	20 U	20.8	0.31	0.17	0.85	± 0.24
		20.6				
		21.2				
T77	113 Th	113.8	0.87	0.50	0.45	± 0.87
		112.4				
		112.2				
	30 U	30.7	0.36	0.21	0.67	± 0.36
		30.9				
		31.4				
T78	79 Th	78.5	0.70	0.40	0.51	± 0.70
		79.6				
		78.3				
	60 U	60.5	0.74	0.43	0.70	± 0.74
		61.6				
		60.2				

metal ions was acquired by conducting a fixed EIR (ARS/XAD-2010) weight (0.1 g) with 50 mL of each uranium (pH 4) and thorium (pH 2) ions solution in perchloric acid (0.01 M) for 10 min contact time at room temperature. Langmuir isotherm model has better fitting experimental data with a maximum adsorption capacity of 20.2 mg g^{-1} for U(VI) and 18.25 mg g^{-1} for Th(IV). The adsorption process of each metal ion by synthesized Alizarin Red S -impregnated XAD-2010 showed an exothermic pseudo-second-order adsorption process. The loaded metal ions were afterward completely eluted using one mole of 10 mL HCl solution using 10 min contact time. The tolerance limits for several metal ions on Alizarin Red S -impregnated XAD-2010 were calculated, giving high tolerance limit. The optimized method was applied to reference and different rock types bearing thorium and uranium with good accurate results.

Compliance with ethical standards

Conflict of interest The authors declare that they have no conflict of interest.

References

1. Agency for Toxic Substances and Disease Registry, U.S. Public Health Service, New York (2008) Health consultation. Depleted uranium at Hawaiian military sites; Schofield Barracks Impact Area; Makua Military Reservation, Pohakuloa Training Area on Islands of Oahu and Hawaii
2. Jain V, Pandya R, Pillai S et al (2006) Solid phase extraction, preconcentration and sequential separation of U(VI), Th(IV), La(III) and Ce(III) by Octa-O-methoxy resorcin[4]arene based Amberlite XAD-4 chelating resin. Talanta 70:257–266. https://doi.org/10.1016/j.talanta.2006.02.032
3. Welz B, Sperling M (1999) Atomic absorption spectrometry. Wiley-VCH, New York

4. Tamborini G (2004) SIMS analysis of uranium and actinides in microparticles of different origin. Microchim Acta 145:237–242. https://doi.org/10.1007/s00604-003-0160-8
5. Dean J (1997) Atomic absorption and plasma spectroscopy. Wiley, London
6. Marczenko Z, Balcerzak M (2000) Separation, preconcentration and spectrophotometry in inorganic analysis, vol 10. Elsevier, Amsterdam
7. Perkampus H (1992) UV–Vis spectroscopy and its applications, vol 33. Springer, Berlin
8. Sengupta A, Ippili T, Jayabun S et al (2016) ICP-AES determination of trace metallic constituents in thorium matrix after preferential extraction of thorium using TBP, TOPO and DHOA: a comparative study. J Radioanal Nucl Chem 310(1):59–67. https://doi.org/10.1007/s10967-016-4790-9
9. Kato K, Ito M, Watanabe K (2000) Determination of thorium and uranium in activated concrete by inductively coupled plasma mass spectrometry after anion-exchange separation. Fresen J Anal Chem 366:54. https://doi.org/10.1007/s002160050011
10. Torgov V, Demidova M, Saprykin A et al (2002) Extraction preconcentration of uranium and thorium traces in the analysis of bottom sediments by inductively coupled plasma mass spectrometry. Anal Chem 57:303. https://doi.org/10.1023/A:1014942112864
11. Tolmachyov S, Kuwabara J, Noguchi H (2004) Flow injection extraction chromatography with ICP-MS for thorium and uranium determination in human body fluids. J Radioanal Nucl Chem 261:125. https://doi.org/10.1023/B:JRNC.0000030945.53499.1c
12. Ghaedi M, Asadpour E, Vafaie A (2006) Simultaneous preconcentration and determination of copper, nickel, cobalt, lead and iron content using a surfactant coated alumina. Bull Chem Soc Jpn 79:432–436. https://doi.org/10.1246/bcsj.79.432
13. Lemos V, David G, Santos L (2006) Synthesis and application of XAD-2/Me-BTAP resin for on-line solid phase extraction and determination of trace metals in biological samples by FAAS. J Braz Chem Soc 17:697–704. https://doi.org/10.1590/S0103-50532006000400010
14. Gupta N, Sengupta A, Gupta A et al (2018) Biosorption-an alternative method for nuclear waste management: a critical review. J Environ Chem Eng 6(2):2159–2175. https://doi.org/10.1016/j.jece.2018.03.021
15. Sengupta A, Gupta N (2017) MWCNTs based sorbents for nuclear waste management: a review. J Environ Chem Eng 5(5):5099–5114. https://doi.org/10.1016/j.jece.2017.09.054
16. Dubey R, Bhalotra A, Gupta M et al (1998) Differential-pulse polarographic-determination of uranium(VI) in standard and synthetic samples after adsorption of its quinolin-8-olate on microcrystalline naphthalene. Anal Chim 88:719–729
17. Seki T, Oguma K (2004) Determination of uranium in natural waters and high-purity aluminum by flow-injection on-line preconcentration and ICP-MS detection. Bunseki Kagaku 53:353–357. https://doi.org/10.2116/bunsekikagaku.53.353
18. Rao T, Metilda P, Mary Gladis J (2006) Preconcentration techniques for uranium(VI) and thorium(IV) prior to analytical determination: an overview. Talanta 68:1047–1064. https://doi.org/10.1016/j.talanta.2005.07.021
19. Ghaedi M, Niknam K, Zamani S et al (2013) Silica chemically bonded N-propyl kriptofix 21 and 22 with immobilized palladium nanoparticles for solid phase extraction and preconcentration of some metal ions. Mater Sci Eng C 33:3180–3189. https://doi.org/10.1016/j.msec.2013.03.045
20. Gladis J, Rao T (2002) Solid phase extractive preconcentration of uranium on to 5,7-dichloroquinoline-8-ol modified naphthalene. Anal Lett 35:501–515. https://doi.org/10.1081/AL-120002683
21. Hosseini M, Hosseini-Bandegharaei A (2011) Comparison of sorption behavior of Th(IV) and U(VI) on modified impregnated resin containing quinizarin with that conventional prepared impregnated resin. J Hazard Mater 190:755–765. https://doi.org/10.1016/j.jhazmat.2011.03.111
22. Hosseini-Bandegharaei A, Hosseini M, Jalalabadi Y et al (2011) A novel extractant- impregnated resin containing carminic acid for selective separation and pre-concentration of uranium(VI) and thorium(IV). Int J Environ Anal Chem 93:108–124. https://doi.org/10.1080/03067319.2011.620706
23. Korn M, Santos A, Jaegera H et al (2004) Copper, zinc and manganese determination in saline samples employing FAAS after separation and preconcentration on Amberlite XAD-7 and Dowex 1X-8 loaded with alizarin red SJ. Braz Chem Soc 15(2):212–218
24. Hosseini M, Bazrafshan A, Hosseini-Bandegharaei A (2016) A novel solvent-impregnated resin containing 3-hydroxy-2-naphthoic acid for stepwise extraction of Th(IV) and U(VI) over other coexistence ions. Sep Sci Technol 51(8):1328–1335. https://doi.org/10.1080/01496395.2016.1147465
25. Soylak M, Elci L, Dogan M (2001) Solid phase extraction of trace metal ions with Amberlite XAD resins prior to atomic absorption spectrometric analysis. J Trace Microprobe Technol 19:329–344. https://doi.org/10.1081/TMA-100105049
26. Lemos V, Nunes L, Baliza P et al (2004) On-line solid phase extraction system for cadmium preconcentration and determination by flame atomic absorption spectroscopy. Can J Anal Sci Spectrosc 49:24–30
27. Qadeer R, Hanif J, Khan M et al (1995) Uptake of uranium ions by molecular sieve. Radiochim Acta 68:197–201
28. Landgraf W, Li N, Benson J (2003) Polymer microcarrier exhibiting zero-order release. Drug Deliv Technol 3:1–12
29. Sigma-Aldrich (2006) Amberlite XAD polimeric resins. http://www.sigmaaldrich.com/sigma/product%20information%20sheet/xad7pis.pdf. Accessed 10 Aug 2006
30. Bulut V, Duran C, Tufekci M et al (2007) Speciation of Cr(III) and Cr(VI) after column solid phase extraction on Amberlite XAD-2010. J Hazard Mater 143:112–117. https://doi.org/10.1016/j.jhazmat.2006.08.074
31. Duran C, Gundogdu A, Bulut V et al (2007) Separation and enrichment of gold(III) from environmental samples prior to its flame atomic absorption spectrometric determination. J Hazard Mater 149:317–323. https://doi.org/10.1016/j.jhazmat.2007.03.083
32. Duran C, Senturk H, Gundogdu A et al (2007) Determination of some trace metals in environmental samples by flame AAS following solid phase extraction with Amberlite XAD-2000 resin after complexing with 8-hydroxyquinoline. Chin J Chem 25:196–202. https://doi.org/10.1002/cjoc.200790040
33. Hosseini M, Hosseini-Bandegharaei A (2010) Selective extraction of Th(IV) over U(VI) and other co-existing ions using eosin B impregnated Amberlite IRA-410 resin beads. J Radioanal Nucl Chem 283:23–30. https://doi.org/10.1007/s10967-009-0037-3
34. Hosseini M, Hosseini-Bandegharaei A, Raissi H et al (2009) Sorption of Cr(VI) by Amberlite XAD-7 resin impregnated with brilliant green and its determination by quercetin as a selective spectrophotometric reagent. J Hazard Mater 169:52–57. https://doi.org/10.1016/j.jhazmat.2009.03.058
35. Hosseini M, Hosseini-Bandegharaei A, Hosseini M (2009) Column-mode separation and pre-concentration of some heavy metal ions by solvent-impregnated resins containing quinizarin before the determination by flame atomic absorption spectrometry. Int J Environ Anal Chem 89:35–48. https://doi.org/10.1080/03067310802464948
36. Hosseini-Bandegharaei A, Hosseini M, Jalalabadi Y (2011) Removal of Hg(II) from aqueous solutions using a novel

impregnated resin containing 1-(2-thiazolylazo)-2-naphthol (TAN). Chem Eng J 168:1163–1173. https://doi.org/10.1016/j.cej.2011.02.004
37. Hosseini-Bandegharaei A, Hosseini M, Sarw-Ghadi M et al (2010) Kinetics, equilibrium and thermodynamic study of Cr(VI) sorption into toluidine blue o-impregnated XAD-7 resin beads and its application for the treatment of wastewaters containing Cr(VI). Chem Eng J 160:190–198. https://doi.org/10.1016/j.cej.2010.03.040
38. Marczenko Z (1986) Separation and spectrophotometric determination of elements, vol 60. Wiley, New York
39. Leenheer A, Ruyter M, Steyaert H (1976) A method for the statistical evaluation of results in external quality control surveys. Clin Chim Acta 71:229–238. https://doi.org/10.1016/0009-8981(76)90535-0
40. Davis J (1986) In: Handbook of statistics and analysis in geology, 2nd edn. Wiley, New York, p 646
41. Christian G (1994) In: Handbook of analytical chemistry, 5th edn, chapter 2. Wiley, New York, pp 22–26
42. Muraviev D (1998) Surface impregnated sulfonate ion exchangers: preparation, properties and application. Solvent Extr Ion Exch 16:381–457. https://doi.org/10.1080/07366299808934533
43. Muraviev D, Ghantous L, Valiente M (1998) Stabilization of solvent-impregnated resin capacities by different techniques. React Funct Polym 38:259–268. https://doi.org/10.1016/S1381-5148(98)00075-3
44. Hosseini-Bandegharaei A, Sarwghadi M, Heydarbeigi A et al (2013) Solid-phase extraction of trace amounts of uranium(VI) in environmental water samples using an extractant-impregnated resin followed by detection with UV-Vis spectrophotometry. J Chem 2013:1–10. https://doi.org/10.1155/2013/671564
45. Maihub A, El-ajaily M, Aboukrish M et al (2003) Synthesis and characterization of some homodinuclear mixed ligand complexes of Co(II) and Cu(II) part II. Jerash Res Stud 7(2):41–47
46. Khalifa M (1998) Selective separation of uranium using Alizarin Red S (ARS)-modified anion-exchange resin or by flotation of U-ARS chelate. Sep Sci Technol 33:2123–2141. https://doi.org/10.1080/01496399808545719
47. Wang G, Liu J, Wang X et al (2009) (Adsorption of uranium(VI) from aqueous solution onto cross-linked chitosan. J Hazard Mater 168:1053–1058
48. Anirudhan T, Rijith S (2012) Synthesis and characterization of carboxyl terminated poly(methacrylic acid) grafted chitosan/bentonite composite and its application for the recovery of uranium(VI) from aqueous media. J Environ Radioact 106:8–19. https://doi.org/10.1016/j.jenvrad.2011.10.013
49. Atrees E, Metwally B, Demerdash M et al (2016) Sorption behavior of Pr and Nd upon chitosan benzoyl thiourea derivatives. J Radiat Res Appl Sci 9:207–216
50. Kalal H, Panahi H, Hoveidi H et al (2012) Synthesis and application of Amberlite XAD-4 functionalized with alizarin red-s for preconcentration and adsorption of rhodium(III). Iran J Environ Health Sci Eng 9:1–9
51. Cheira M, Atia B, Kouraim M (2017) Uranium(VI) recovery from acidic leach liquor by Ambersep 920U SO_4 resin: kinetic, equilibrium and thermodynamic studies. J Radiat Res Appl Sci 10:307–319
52. Pakade V, Cukrowska E, Darkwa J et al (2012) Simple and efficient ion imprinted polymer for recovery of uranium from environmental samples. Water Sci Technol 65:728–736
53. Zhang H, Liang H, Chen Q et al (2013) Synthesis of a new ionic imprinted polymer for the extraction of uranium from seawater. J Radioanal Nucl Chem 298:1705–1712. https://doi.org/10.1007/s10967-013-2612-x
54. Li F, Li D, Li X et al (2016) Microorganism derived carbon microspheres for uranium removal from aqueous solution. Chem Eng J 284:630–639
55. Hosseini S, Rahmani-Sani A, Jalalabadi Y et al (2015) Preconcentration and determination of ultra-trace amounts of U(VI) and Th(IV) using titan yellow impregnated Amberlite XAD-7 resin. Int J Environ Anal Chem 95:277–290. https://doi.org/10.1080/03067319.2015.1016009
56. Baes J, Mesmer R (1976) Hydrolysis of cations. Wiley, New York
57. Elsalamouny A, Desouky O, Mohamed S et al (2016) Evaluation of adsorption behavior for U(VI) and Th(IV) ions onto solidified mannich type material. J Dispers Sci Technol 38:860–865. https://doi.org/10.1080/01932691.2016.1207546
58. Atia A (2005) Studies on the interaction of mercury(II) and uranyl(II) with modified chitosan resins. Hydrometallurgy 80:13–22. https://doi.org/10.1016/j.hydromet.2005.03.009
59. Li W, Tao Z (2002) Biosorption of americium-241 by Saccharomyces cerevisiae. J Radioanal Nucl Chem 254:187–191. https://doi.org/10.1023/A:1015276813386
60. Mishra S, Achary G, Das M (2012) Adsorption of Cu(II) by used aqua guard carbon(UAC). J Chem Pharm Res 4(2):1207–1216
61. Sharma I, Goyal D (2009) Kinetic modeling: chromium(III) removal from aqueous solution bymicrobial waste biomass. J Sci Ind Res 68:640–646
62. Ho Y, McKay G (1999) Pseudo-second order model for sorption processes. Process Biochem 34:451–465. https://doi.org/10.1016/S0032-9592(98)00112-5
63. Lagergren S (1898) About the theory of so-called adsorption of soluble substance. Kungliga Svenska Vetenskapsakademiens Handlingar 24:1–39
64. Donia A, Atia A, Daher A et al (2011) Selective separation of U(VI) from its solutions using amine modified silica gel produced from leached zircon. Int J Miner Process 101:81–88
65. Weber W, Morris J (1963) Kinetics of adsorption on carbon from solution. J Sanit Eng Div Proc 89:31–59
66. Preetha C, Rao T (2006) Preconcentration of uranium(VI) by solid phase extraction onto dicyclohexano-18-crown-6 embedded benzophenone. J Radioanal Nucl Chem 267:265–270. https://doi.org/10.1007/s10967-006-0042-8
67. Preetha C, Gladis J, Rao T (2002) Solid phase extractive preconcentration of thorium onto 5,7-dichloroquinoline-8-ol modified benzophenone. Talanta 58:701–709. https://doi.org/10.1016/S0039-9140(02)00378-8
68. Gladis J, Rao J (2002) Quinoline-8-ol-immobilized Amberlite XAD-4: synthesis, characterization, and uranyl ion uptake properties suitable for analytical applications. Anal Bioanal Chem 373:867–887. https://doi.org/10.1007/s00216-002-1387-7.12194052
69. Jain V, Handa A, Sait S et al (2001) Pre-concentration, separation and trace determination of lanthanum(III), cerium(III), thorium(IV) and uranium(VI) on polymer supported o-vanillinsemicarbazone. Anal Chim Acta 429:237–246. https://doi.org/10.1016/S0003-2670(00)01299-X
70. Kumar M, Rathore D, Singh A (2001) Pyrogallol immobilized Amberlite XAD-2: a newly designed collector for enrichment of metal ions prior to their de-termination by flame atomic absorption spectrometry. Mikrochim Acta 137:127–134. https://doi.org/10.1007/s006040170002
71. Jal P, Dutta R, Sudershan K (2001) Extraction of metal ions using chemically modified silica gel: a PIXE analysis. Talanta 55:233–240. https://doi.org/10.1016/S0039-9140(00)00678-0
72. Kumar M, Rathore D, Singh A (2000) Metal ion enrichment with Amberlite XAD-2 functionalized with Tiron: analytical applications. Analyst 125:1221–1226. https://doi.org/10.1039/b000858n

73. Prabhakaran D, Subramanian M (2004) Selective extraction of U(VI), Th(IV), and La(III) from acidic matrix solutions and environmental samples using chemically modified Amberlite XAD-16 resin. Anal Bioanal Chem 379:519–525. https://doi.org/10.1007/s00216-004-2600-7
74. Hosseini M, Hosseini M, Bandeh-Gharaei A (2007) Solvent impregnated resins containing quinizarin: preparation and application to batch-mode separation of Cd(II), Cu(II), Ni(II), and Zn(II) in aqueous media prior to the determination by flame atomic absorption spectrometry. Sep Sci Technol 42:3465–3480. https://doi.org/10.1080/01496390701626552
75. Ummathur M, Malini P, Krishnankutty K (2013) Dioxouranium(VI) complexes of some unsaturated β-diketones. Int J Chem Technol Res 5:1–5
76. Foo K, Hameed B (2010) Insights into the modeling of adsorption isotherm systems. Chem Eng J 156:2–10. https://doi.org/10.1016/j.cej.2009.09.013
77. Aksoyoglu S (1989) Sorption of U(VI) on granite. J Radioanal Nucl Chem 134:393–403
78. Chen A, Chen S (2009) Biosorption of azo dyes from aqueous solution by glutaraldehyde-crosslinked chitosans. J Hazard Mater 172:1111–1121
79. Kundu S, Gupta A (2006) Arsenic adsorption onto iron oxide-coated cement (IOCC): regression analysis of equilibrium data with several isotherm models and their optimization. Chem Eng J 122:93–106
80. Zhang X, Jiao C, Wang J et al (2012) Removal of uranium) VI) from aqueous solutions by magnetic schiff base: kinetic and thermodynamic investigation. Chem Eng J 198–199:412–419
81. Lima E, Hosseini-Bandegharaei A, Moreno-Piraján J et al (2019) A critical review of the estimation of the thermodynamic parameters on adsorption equilibria. Wrong use of equilibrium constant in the Van't Hoof equation for calculation of thermodynamic parameters of adsorption. J Mol Liq 273:425–434
82. Elsalamouny A, Desouky O, Mohamed S et al (2017) Evaluation of adsorption behavior for U(VI) and Nd(III) ions onto fumarated polystyrene microspheres. J Radioanal Nucl Chem 314:429–437. https://doi.org/10.1007/s10967-017-5389-5
83. Khawassek Y, Masoud A, Taha M et al (2018) Kinetics and thermodynamics of uranium ion adsorption from waste solution using Amberjet 1200 H as cation exchanger. J Radioanal Nucl Chem 315:493–502. https://doi.org/10.1007/s10967-017-5692-1
84. Orabi A, Atrees M, Salem H (2018) Selective preconcentration of uranium on chitosan Steroyl thiourea prior to its spectrophotometric determination. Sep Sci Technol 53(14):2267–2283. https://doi.org/10.1080/01496395.2018.1445113
85. Cheira M (2015) Synthesis of pyridylazo resorcinol-functionalized Amberlite XAD-16 and its characteristics for uranium recovery. J Environ Chem Eng 3:642–652. https://doi.org/10.1016/j.jece.2015.02.003
86. Afifi S, Mustafa M, El Sheikh E et al (2012) Extraction and determination of thorium and its application on geologic samples using trioctyl phosphine oxide. Arab J Nucl Sci Appl 45(3):1–16
87. Fouad H, Abu Elenein S, Elrakaiby R et al (2015) A developed spectrophotometric method for thorium determination using Alizarin Red S Dye in different types of its bearing rocks. Int J Sci Res 4:1611–1615
88. Bale M, Sawant A (2011) Solvent extraction and spectrophotometric determination of uranium(VI) with pyridine- 2-carboxaldehyde 2-hydroxybenzoylhydrazone. J Radioanal Nucl Chem 247:531–534. https://doi.org/10.1023/A:1010626409358